Drug Design, Development and Therapy

Dovepress
Taylor & Francis Group

Open Access Full Text Article

ORIGINAL RESEARCH

Integrative Network Pharmacology and Transcriptomics Reveal the Mechanism of Gui-Qi-Yi-Shen Granules in the Treatment of IgA Nephropathy

Jia-Wei Cao[1], Yue-Wen Tang[1,2], Meng-Ya Jiang[1], Meng-Dan Lu[3], Ru-Chun Yang[1,4], Dong-Rong Yu[1,4], Feng Wan[1,4]

[1]Department of Nephrology, Hangzhou TCM Hospital Affiliated to Zhejiang Chinese Medical University, Hangzhou, People's Republic of China; [2]Department of Nephrology, Hangzhou Dingqiao Hospital, Hangzhou, People's Republic of China; [3]College of Life Sciences, Zhejiang Chinese Medical University, Hangzhou, People's Republic of China; [4]Zhejiang Key Laboratory of Blood-Stasis-Toxin Syndrome, Zhejiang Chinese Medical University, Hangzhou, People's Republic of China

Correspondence: Dong-Rong Yu; Feng Wan, Hangzhou TCM Hospital Affiliated to Zhejiang Chinese Medical University, Hangzhou, 310007, Tiyuchang Road 453, People's Republic of China, Tel +86-571-88950659, Email yudr68@163.com; wfthebest@163.com

Background: IgA nephropathy (IgAN) is a significant contributor to kidney failure and death, with limited therapeutic options. Gui-qi-yi-shen (GQYS) granules are a classic Chinese medicine prescription for treating IgAN. Nevertheless, the underlying molecular mechanism is still unclear.

Purpose: To elucidate the mechanism by which GQYS exerts its therapeutic effects in IgAN treatment.

Materials and Methods: Itgam-IRES-hCD89 mice (eight-week-old) were divided into four groups: IgAN, low-dose GQYS (GQYS-L, 5.2 g/kg), high-dose GQYS (GQYS-H, 10.4 g/kg), and Losartan (6.5 mg/kg). Coincident C57/BL6 mice were used as controls. Periodic acid-Schiff (PAS) staining, biochemical analyses, and immunofluorescence (IF) were used for therapeutic evaluation. Network pharmacology and transcriptomic analyses were performed to investigate the potential mechanisms of GQYS, while Western blotting and IF were performed to confirm these actions.

Results: Compared to the model group, 24 h proteinuria and alanine aminotransferase levels were significantly reduced in the GQYS groups. PAS staining showed that IgAN mice exhibited glomerular mesangial hypercellularity as well as matrix expansion, whereas these pathologies were alleviated in the GQYS groups. IF results revealed that GQYS reduced deposition of IgA and C3 in the glomerular mesangial areas compared to that in the model mice. Network pharmacology and transcriptomic analyses identified genes and pathways that may be associated with the effects of GQYS against IgAN. Western blotting and IF results indicated GQYS attenuated the expression of TLR4/MyD88/NF-kB and IL-6/JAK2/STAT3 signaling pathway related proteins.

Conclusion: GQYS reduced proteinuria and ameliorate renal pathological damage in IgAN via TLR4/MyD88/NF-kB and IL-6/JAK2/STAT3 signaling, offering a promising therapeutic strategy.

Keywords: IgA nephropathy, Gui-qi-yi-shen granules, renoprotection, TLR4 signaling pathway, IL-6 signaling pathway

Introduction

IgA nephropathy (IgAN) ranks as the most common primary glomerulonephritis globally. Within 20–25 years following diagnosis, roughly 30–45% of patients with IgAN will advance to end-stage renal disease (ESRD).[1] In the past, IgAN treatment mainly relied on supportive care. Immunosuppressive therapy, despite its effectiveness, was limited by side effects. Recently, several new targeted drugs have been approved for IgAN treatment, including SGLT-2 inhibitors, gut-targeted budesonide (Nefecon), endothelin receptor antagonists, and complement inhibitors.[2,3] Existing treatments, however, still have many limitations in terms of efficacy, side effects, and applicability. Therefore, there is an urgent need to seek effective intervention measures to delay the progression of IgAN, and in turn reduce the occurrence of

Received: 23 April 2025
Accepted: 12 July 2025
Published: 22 July 2025

ESRD. Clinical practice has indicated that traditional Chinese medicine has activity in reducing proteinuria, and alleviating kidney inflammation and fibrosis in patients with chronic kidney disease.[4,5]

Gui-qi-yi-shen (GQYS) granules, derived from compound Centella asiatica, are a clinical prescription developed by the Chinese medical master, Yongjun Wang. This formula comprises five traditional Chinese medicines: Centella asiatica (L). Urban (Jixuecao), Astragalus membranaceus (Fisch). Bunge (HuangQi), Rheum officinale Baill (DaHuang), Semen Persicae (TaoRen), and Angelica sinensis (Oliv). Diels (DangGui) (China Patent Application number: 200510048997.9), which has been approved for the hospital preparation (ZheYaoZhibeiZi: Z20240001000). The formula is based on the principles of nourishing qi and blood, resolving blood stasis, eliminating symptoms, and dispelling wind and dampness, which coincide with the main syndrome and pathogenesis of IgAN. The clinical treatment of IgAN with GQYS has yielded positive therapeutic effects;[6,7] nevertheless, the associated specific mechanism of its action requires in-depth basic research to fully elucidate.

In this study, we explored the effects of GQYS on IgAN using Itgam-IRES-hCD89 transgenic mice, which can simulate the pathological features of human IgAN, including IgA deposition in the glomerular mesangial area, expansion of the mesangial matrix, and mild proteinuria, similar to the classic CD89 transgenic mice.[8,9] Through combining network pharmacology, transcriptomic analysis, and experimental validation, we found that GQYS prevents kidney injury in mice with IgAN mainly through suppressing the TLR4/MyD88/NF-kB and IL-6/JAK2/STAT3 signal transduction pathways. The flow chart of the study is shown in Figure 1. All the steps and results of the component analysis, network pharmacology and pharmacodynamic experiments are presented in this figure.

Materials and Methods

Reagents and Drugs

GQYS were provided by the TCM Pharmacy of Hangzhou hospital of Traditional Chinese Medicine. Losartan potassium tablets were provided by Merck Sharp & Dohme Limited (approval number: HJ20171081, Hangzhou).

The other materials included: Periodic Acid-Schiff (PAS) stain kit (G1281, Lot: No.2306001, Solarbio), Alexa Fluor® 488-conjugated goat anti-mouse IgA (1040–30, SouthernBiotech, Birmingham, AL, USA), FITC-conjugated goat anti-mouse C3

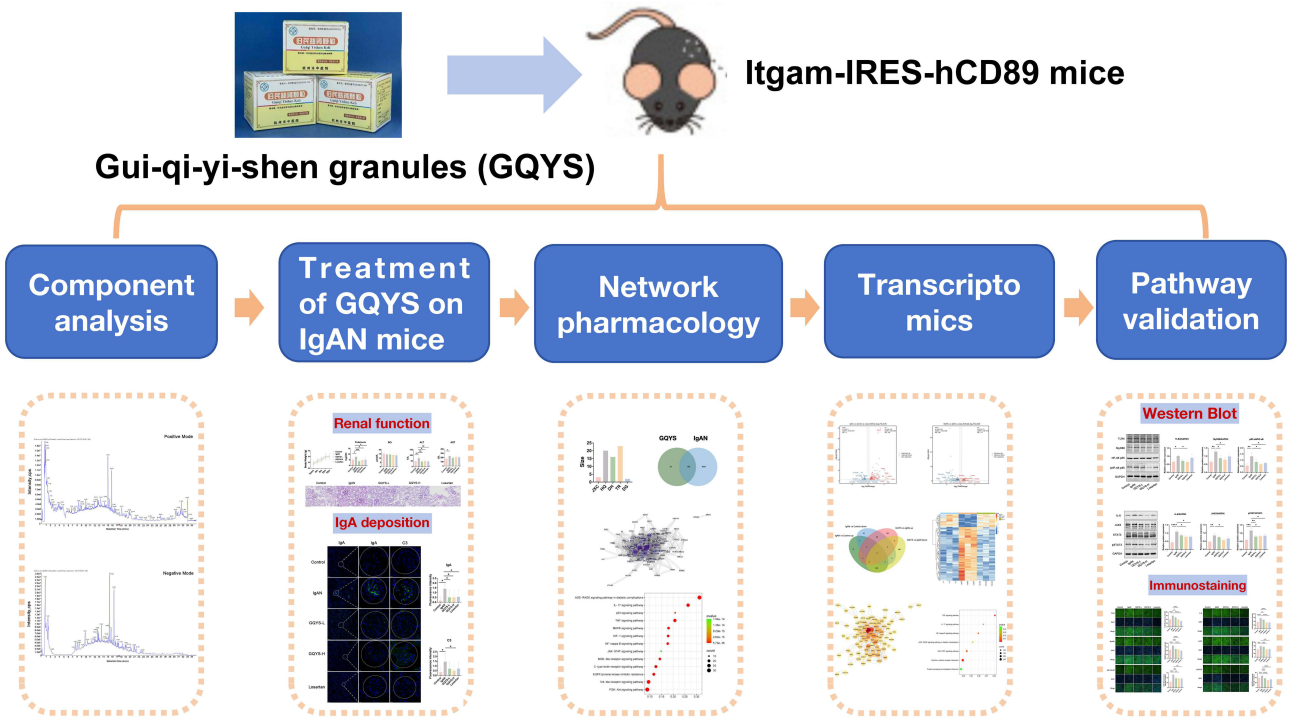

Figure 1 Flow chart showing the detailed process of this study.

(0855500, MP Biomedicals, Irvine, CA, USA). The antibodies used were as follows: TLR4 (19,811-1-AP, Proteintech), NF-kB p65 (10,745-1-AP, Proteintech), phospho-NF-kB p65 (10,745-1-AP, Proteintech), MyD88 antibody (ab219413, Abcam), IL-6 (A0286, Abclonal), JAK2 (ET1607-35, HUABIO), STAT3 (AF1492, Beyotime), phospho-STAT3 (ET-1607-39, HUABIO), GAPDH (60004-1-Ig, Proteintech), Goat anti-rabbit /mouse IgG Secondary Antibody (926–32,210/926-68071, LI-COR, USA), Alexa Fluor™ Plus 488 conjugated donkey anti-rabbit IgG (H+L) (Invitrogen, A32790), and DAPI (ab104139, Abcam).

Component Analysis

The chemical constituents of GQYS were identified by ultra-high-performance liquid chromatography coupled with quadrupole time-of-flight mass spectrometry (UPLC-Q-TOF-MS/MS). Briefly, the GQYS granules (1 g) were accurately weighed, dissolved in ultrapure water, and diluted to 20 mg/mL. The solution was then filtered through a 0.22 μm membrane filter and injected for analysis. The electrospray ionization (ESI) was used as the ionization source by 7600 ZenoTOF High Definition Mass Spectrometer (AB Sciex, USA). The separation was performed by a Waters ACQUITY UPLC Cortecs T3 Column (2.1× 100 mm, 1.6μm) with Cortecs T3 Van Guard (2.1×50 mm, 1.6 μm). The MS analysis utilized an ESI source with an acquisition range of 50–1500 Da. Each sample was injected 5μL into the column and employed with a gradient elution. The column and autosampler temperature were maintained at 50 °C and 4 °C. The gradient elution consisted of acetonitrile and 0.1% formic acid in water, the flow rate was controlled at 0.35 mL/min.

Animals and Treatments

Eight-week-old male Itgam-IRES-hCD89 mice (n=40, Cat. NO. NM-KI-200063) were procured from the Shanghai Model Organisms Center, Inc. Male C57BL/6 mice of the same age were used as the controls (n=10). Mice were maintained and bred in a specific pathogen-free environment. Approval for all experiments was obtained from the Animal Research Committee of Zhejiang Chinese Medical University (approval number: IACUC-20240311-07). Animal experiments were conducted by the National Institutes of Health guidelines on the use of experimental animals.

After 1 week of adaptation, the Itgam-IRES-hCD89 mice were allocated into four groups: IgAN (IgAN), low-dose GQYS (GQYS-L), high-dose GQYS (GQYS-H), and losartan (Losartan), with 10 mice in each group. The GQYS-L and GQYS-H groups were administered 5.2 and 10.4 g/kg GQYS by gavage, respectively. The dose of GQYS-L group was equivalent to the human clinical dose (40 g/day in adults), and the GQYS-H group received twice this dose. Mice in the Losartan group were administered a 6.5 mg/kg losartan potassium suspension. These doses were calculated based on clinically used doses converted from body surface area.[10] The intervention lasted for 5 months. Lastly, all the mice were sacrificed; serum creatinine (Scr), 24 h proteinuria, and other biochemical indicators were determined using a Chemistry Analyzer (Beckman Coulter, Brea, CA, USA). Kidneys were collected for further analyses.

PAS Staining

Kidney tissues were immersed in 10% formalin solution overnight, followed by embedding in paraffin. Subsequently, they were sectioned into slices with a thickness of 2 μm, and stained with PAS. Next, images were obtained using a slide-scanning system (KF-PRO-020-HI; Konfoong Bioinformation Tech Co., Ltd., Zhejiang, China).

Network Pharmacology Analysis

The compounds in GQYS along with their respective targets were retrieved through a search of the Traditional Chinese Medicine Systems Pharmacology and Analysis Platform (TCMSP) database (https://old.tcmsp-e.com/tcmsp.php). Disease targets associated with IgAN were gathered from three databases, namely GeneCards (https://www.genecards.org), DisGeNET (https://www.disgenet.org/), and OMIM (https://www.omim.org). A Venn diagram was created using the jvenn online website (https://jvenn.toulouse.inrae.fr/app/example.html). The herb-compound-target network was built utilizing Cytoscape 3.7.2. PPI network was obtained by the STRING database (http://string-db.org/), then visualized using Cytoscape software.

Transcriptome Analyses

Kidney tissues were rapidly ground in liquid nitrogen. Total RNA was extracted using TRIzol reagent according to the manufacturer's protocol. RNA purity and quantification were evaluated using the NanoDrop 2000 spectrophotometer (Thermo Scientific, USA). RNA integrity was assessed using the Agilent 2100 Bioanalyzer (Agilent Technologies, Santa Clara, CA, USA). Then the libraries were constructed using VAHTS Universal V6 RNA-seq Library Prep Kit according to the manufacturer's instructions.

The RNA sequencing is performed by OE Biotech, Inc. (Shanghai, China). Initial quality control of the raw fastq files was performed with FastQC (v0.11.9). The clean reads were mapped to the reference genome using HISAT2 (2.1.0). FPKM3 of each gene was calculated and the read counts of each gene were obtained by HTSeq-count (0.11.2). Differential expression analysis was performed using the DESeq2 (1.22.2). Q value < 0.05 and the log2 fold change > 1.2 were set as the threshold for significantly differentially expressed genes (DEGs).

Data analysis was completed using the OECloud tools (https://cloud.oebiotech.com). The original data for transcriptome has been submitted to NCBI's GEO database (GSE286126).

Immunofluorescence Analysis

Frozen kidney sections (3 μm) were stained with Alexa Fluor® 488-conjugated or FITC-conjugated goat antibodies specific for mouse IgA and C3. The pictures were captured using a confocal microscope (STELLARIS 5, Leica, Germany) and scored double-blind by a pathologist using a fluorescent microscope (DM2000 LED, Leica, Germany) (n≥6).

For signaling pathway detection associated proteins, 3 μm paraffin sections were incubated with antibodies including TLR4, MyD88, pNF-kB, IL-6, JAK2, and pSTAT3. The Alexa Fluor™ Plus 488 conjugated secondary antibody was employed. After nuclear staining with DAPI, the sections were observed using a high-content analysis system (Operetta CLS, PerkinElmer, UK) and analyzed using ImageJ software (n=6).

Western Blotting

Kidney proteins were homogenized in cold RIPA buffer, subsequently separated by 10% or 15% SDS-PAGE, and then transferred onto nitrocellulose membranes. After incubation with primary and secondary antibodies, the protein bands were detected by an Odyssey Scanner (LI-COR Biosciences, Lincoln, NE, USA). Quantitative analysis of the bands was then conducted using ImageJ software (version 1.52p) (n=6).

Statistical Analysis

Data analysis was performed using GraphPad Prism software (version 8.0.1). The results are presented as the mean ± standard deviation. To compare multiple groups, one-way analysis of variance was utilized, with $p < 0.05$ indicating statistical significance.

Results

Component Analysis of GQYS

To identify the chemical composition of GQYS, UPLC-Q-TOF-MS/MS analysis was conducted. The total ion chromatograms obtained in both positive and negative ion modes are presented in Figure 2. As listed in Table S1 and S2, 91 components were identified in GQYS.

GQYS Prevented Kidney Injury in Mice with IgAN

During the entirety of the experiment, the body weight of mice in each group did not alter remarkably (Figure 3A), indicating that GQYS was relatively safe. The levels of 24 h proteinuria, alanine aminotransferase (ALT), and aspartate aminotransferase (AST) were elevated significantly in mice with IgAN compared to those in control mice (Figure 3B, D and E). Obvious reductions were observed in the levels of 24 h proteinuria and ALT in the GQYS-L, GQYS-H, and Losartan groups compared to the model group (Figure 3B and D). SCr levels did not change significantly in these groups (Figure 3C). PAS staining

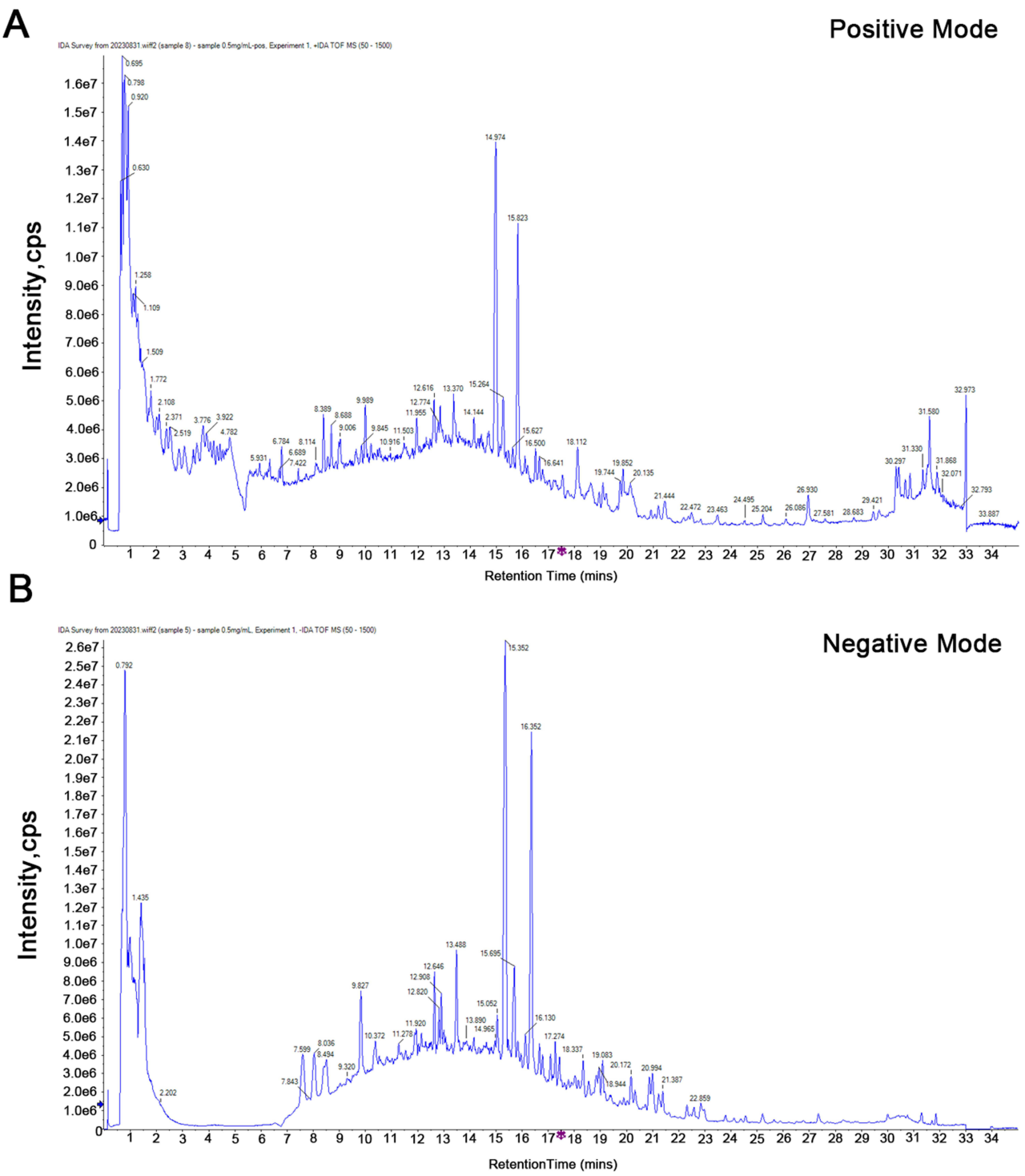

Figure 2 Total ion chromatograms (TIC) of GQYS in positive ion mode (**A**) and negative ion mode (**B**).

revealed that mice with IgAN exhibited increased number of glomerular mesangial cells and expansion of the mesangial matrix; however, these pathological injuries were prominently alleviated in the GQYS-L, GQYS-H, and Losartan groups (Figure 3F). These results indicate that GQYS has a renoprotective effect.

https://doi.org/10.2147/DDDT.S526706

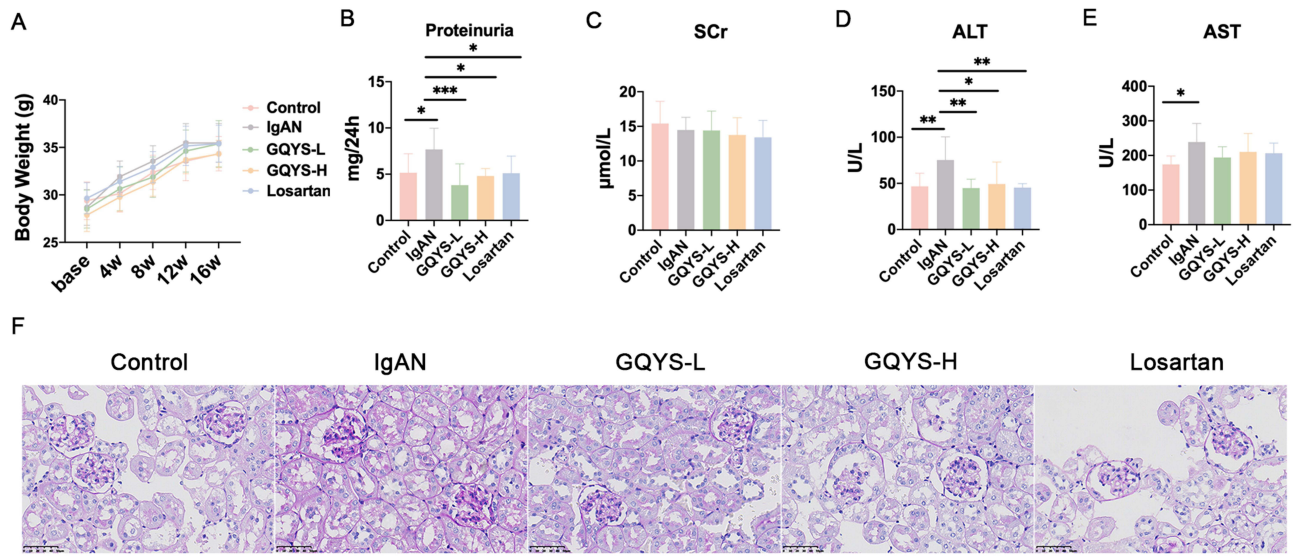

Figure 3 GQYS protects kidney injury in IgAN mice. (**A**) The body weight of mice across various groups were recorded during the experiment course (n=10 for each group). (**B**) The 24 h proteinuria in different groups (n=10). (**C**) SCr level in each group (n=10). (**D**) ALT level in each group (n=10). (**E**) AST level in each group (n=10). Data are presented as mean ± SD. The p-value indicates the statistical significance of each versus the IgAN group. *p < 0.05, **p < 0.01, ***p < 0.001. (**F**) Representative photomicrographs of PAS staining (× 400 magnification) in each group. Scare bar: 100 μm.

GQYS Decreased IgA Deposition in the Mesangial Area of Mice with IgAN

As shown in Figure 4, in mice with IgAN, there was a significant accumulation of granular deposits of IgA in the glomerular mesangial regions (Figure 4A). Compared to the model group, IgA deposition was remarkably reduced in the GQYS-L, GQYS-H, and Losartan groups (Figure 4A and B). Similarly, we also observed C3 deposition in the glomerular mesangial area among mice suffering from IgAN. The deposition of C3 decreased markedly in those intervention groups (Figure 4A and B). These results suggest that GQYS reduces glomerular mesangial deposition of IgA.

Network Pharmacology of GQYS Active Compounds and Related Targets

Sixty-four active compounds from five herbs—Jixuecao, HuangQi, DaHuang, DangGui, and TaoRen—were obtained from the TCMSP database. The screening process resulted in the identification of 3, 20, 16, 23, and 2 active compounds from each respective herb (Figure 5A). No corresponding targets were identified among the 15 active compounds in the TCMSP database. Overall, 45 unique active compounds were analyzed after deduplication (Table S3). In total, 214 unique targets were identified and a herb-compound target network was constructed to visualize their interactions (Figure S1). The network was made up of 268 nodes and 889 edges. The compounds with the highest degrees were quercetin (158), kaempferol (58), 7-O-methylisomucronulatol (42), and formononetin (35). These results indicate that these four compounds might serve as crucial constituents of GQYS in the clinical therapy of diseases.

Disease targets of IgAN were collected from GeneCards, OMIM, and DisGeNET databases. A total of 2756 disease targets were identified after eliminating duplicates (Table S4). From obtaining the intersections, 138 GQYS–IgAN targets were identified (Figure 5B and Table S5). Subsequently, a PPI network of 138 targets was constructed, containing 133 nodes and 2428 edges (Figure 5C). We then identified the main signaling pathways involved in IgAN treatment using KEGG analysis. The significant enrichment pathways included PI3K-AKT signaling, AGE-RAGE signaling, Toll-like receptor signaling (TLR), Tumor necrosis factor (TNF) signaling, and nuclear factor-kappa B (NF-kB) signaling (Figure 5D).

Transcriptomics Analysis of Genes and Pathways Relevant to the Impact of GQYS on IgAN

267 DEGs were ultimately detected between the IgAN and control groups, with 196 upregulated and 71 downregulated genes (Figure 6A, Table S6). In addition, there were 503 DEGs between the GQYS and IgAN groups, comprising 171

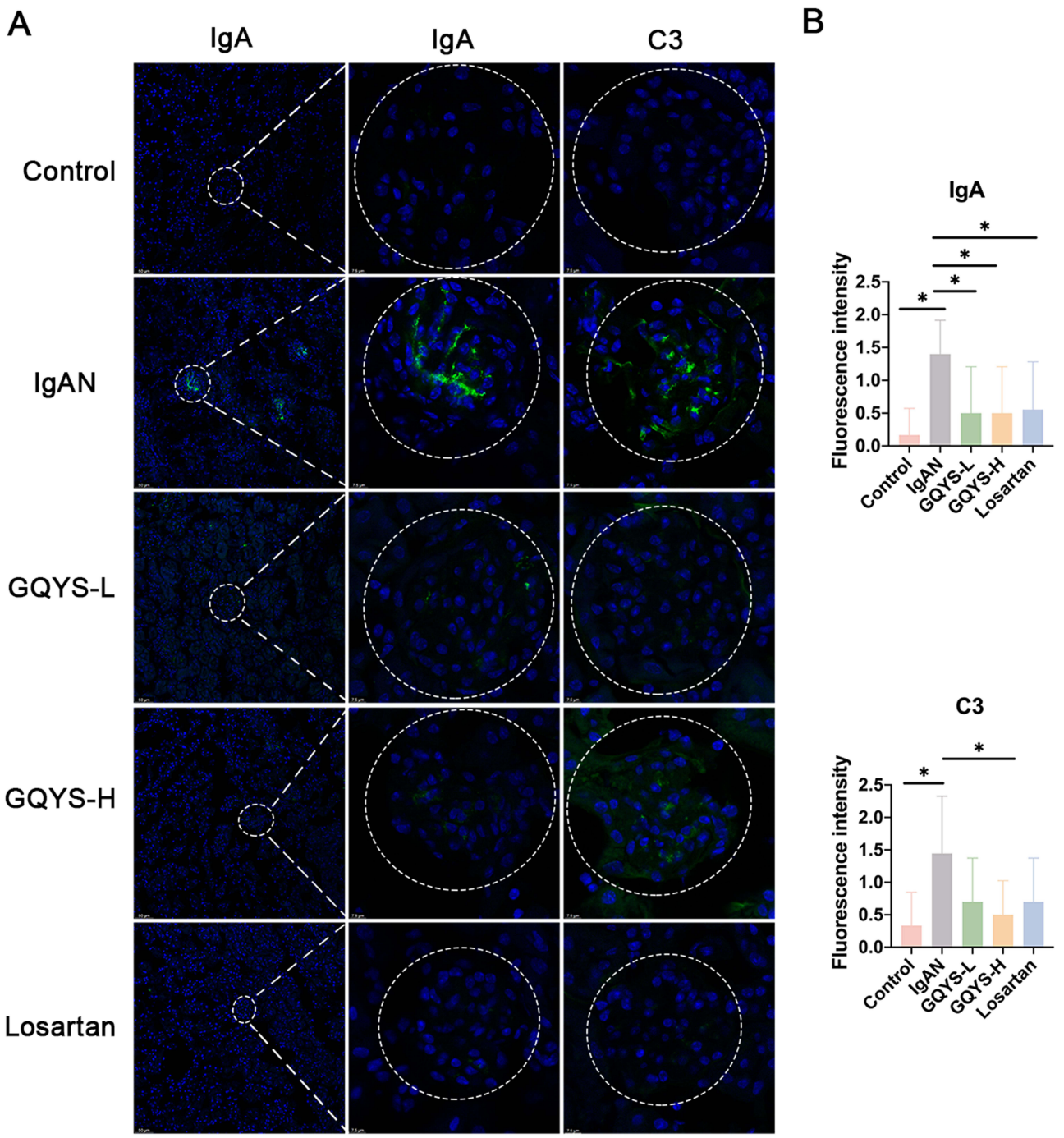

Figure 4 GQYS decreased IgA deposition in the mesangial region of the IgAN mice. (**A**) Immunostaining of IgA and C3 was performed in each group, with nuclei counterstained using DAPI. Scale bars: 50 μm in the left panel, and 7.5 μm in the middle and right panels. (**B**) A professional pathologist blindly assessed and scored the fluorescence intensity (n≥6). Data are presented as mean ± SD. The p-value indicates the statistical significance of each versus the IgAN group. *p < 0.05.

that were upregulated and 332 that were downregulated (Figure 6B, Table S7). Among these, 155 genes exhibited differential expression across all three groups in opposite directions (Figure 6C), and were visualized using heat map analysis (Figure 6D). The PPI network was established based on the STRING database, which contained 94 nodes and 2428 edges (Figure 6E). KEGG analyses showed there was significant enrichment in these pathways, including cytokine-cytokine receptor, JAK-STAT, TNF, and NF-kB signaling (Figure 6F).

https://doi.org/10.2147/DDDT.S526706

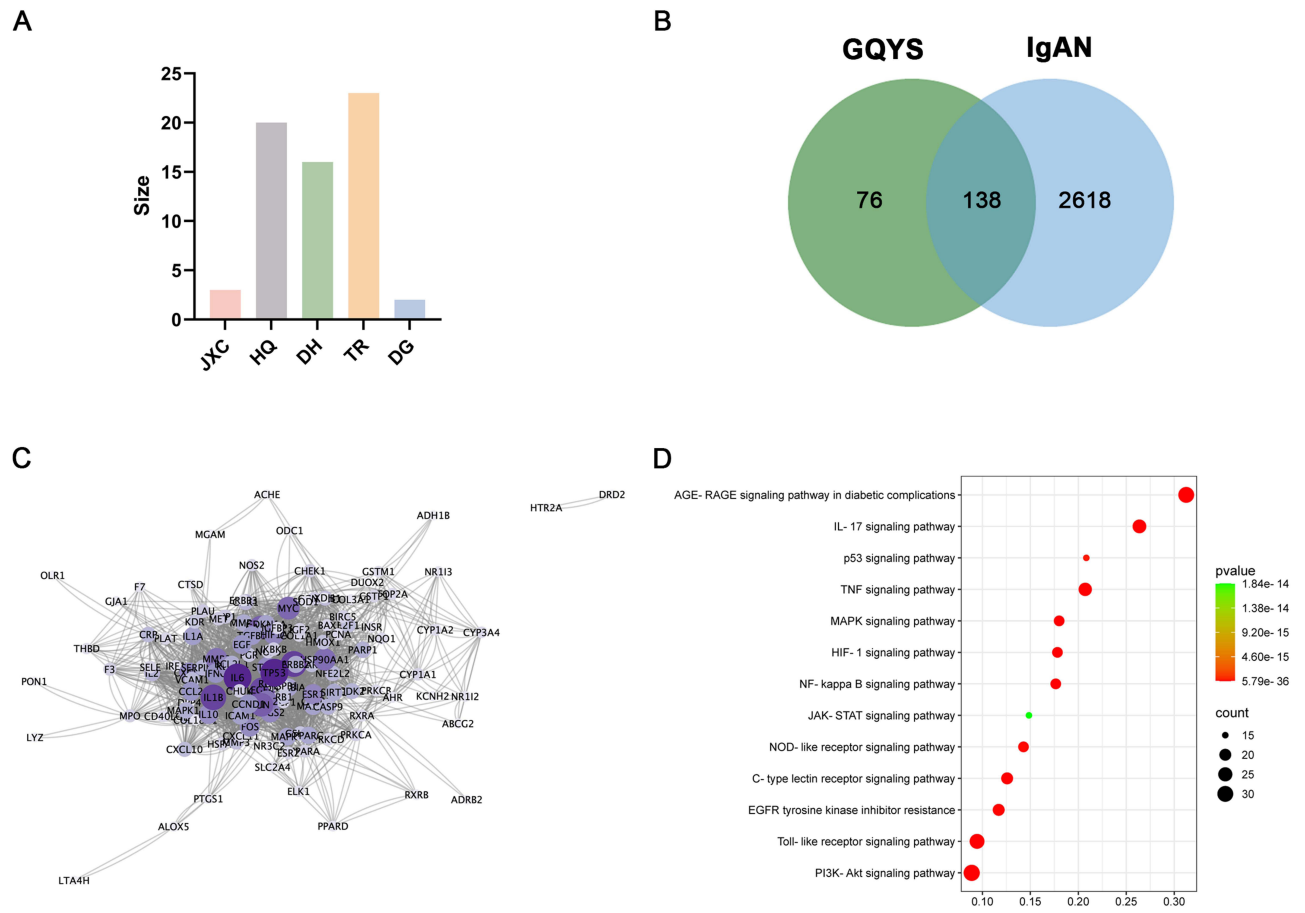

Figure 5 The active compounds and their respective targets of GQYS were examined through network pharmacology analysis. (**A**) Histogram shows the numbers of effective compounds in each herb. (**B**) The Venn diagram depicts the overlapping targets of GQYS and IgAN. (**C**) PPI network based on the common targets. (**D**) The bubble chart visualizing the prominent enrichment pathways.

GQYS Regulated TLR4/MyD88/NF-kB and IL-6/JAK2/STAT3 Signaling Pathways in Mice with IgAN

Based on network pharmacology and transcriptomic analyses, we verified the TLR4/MyD88/NF-kB and IL-6/JAK2/STAT3 signal cascades. IF results showed that TLR4 was mainly distributed in the glomerulus, while MyD88, activated NF-kB, IL-6, JAK2, and activated STAT3 were expressed in both the glomerulus and renal tubules (Figures 7 and 8). Compared to the model groups, the expression of TLR4, MyD88, activated NF-kB, IL-6, JAK2, and activated STAT3 was remarkably decreased in the GQYS groups. Western blotting results showed that the expression of TLR4, MyD88, activated NF-kB, IL-6, JAK2, and activated STAT3 was dramatically increased in IgAN mice, whereas their expression decreased after GQYS intervention (Figures 9 and 10). The results indicated GQYS may regulate TLR4/MyD88/NF-kB and IL-6/JAK2/STAT3 signaling pathways in mice with IgAN.

Discussion

In this study, we used Itgam-IRES-hCD89 mice, similar to CD89 Tg mice developed by Monteiro et al[8,9] CD89 expression in these mice was driven by the CD11b gene promoter. A large amount of mesangial IgA deposition, mesangial matrix dilation, and mild proteinuria spontaneously appeared at 20 weeks. Thus, the Itgam-IRES-hCD89 mice reflected the pathological changes of IgAN and were used to study the effect of GQYS on mesangial IgA deposition and proteinuria.

Traditional Chinese medicine possesses complex polypharmacological properties due to its multi-component, multi-target nature. To better understand how GQYS works in treating IgAN, this study adopted two complementary strategies:

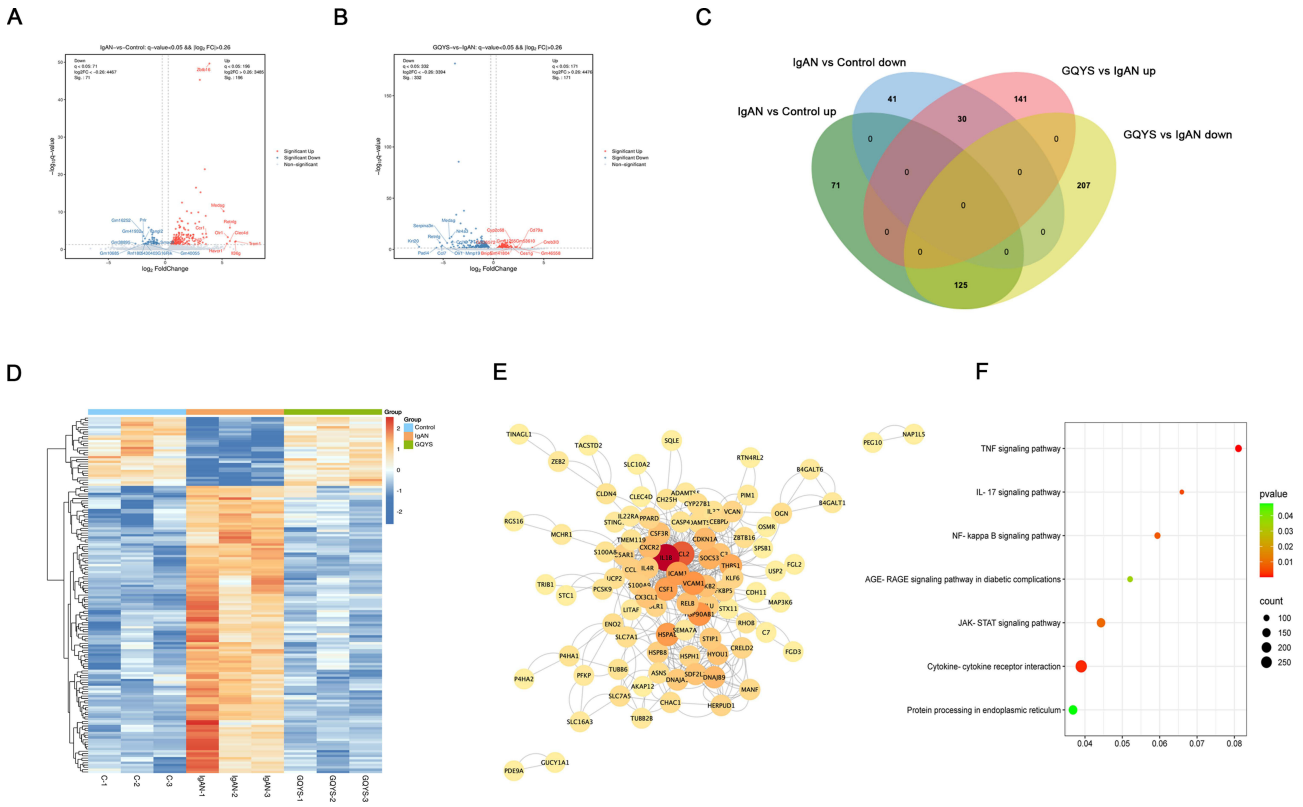

Figure 6 Transcriptomics identified the genes and pathways associated with the therapeutic effect of GQYS on IgAN. (**A**) The volcano plot depicts the DEGs between the control and IgAN groups. (**B**) Volcano plot displays DEGs among the IgAN and GQYS groups. (**C**) Venn diagram of the DEGs among the control, IgAN, and GQYS groups. (**D**) Cluster heatmap showed the DEGs among the control, IgAN, and GQYS groups. (**E**) PPI network of 155 DEGs across all three groups. (**F**) KEGG pathway analysis for 155 DEGs across all three groups.

constituent-oriented and pathway-oriented approaches. Initially, GQYS underwent mass spectrometry to identify its main chemical components. Subsequently, using network pharmacology and the TCMSP database with screening criteria of oral bioavailability≥30% and drug-likeness≥1.8, potential active compounds were selected and cross-analyzed with the mass spectrometry identified components. Three common components were found: kaempferol, formononetin, and rhein. Network analysis showed these three compounds had high degrees, indicating they might be key active components of GQYS for IgAN treatment. Studies have shown their critical roles in modulating inflammatory pathways. For example, kaempferol has significant anti-inflammatory effects, primarily targeting the NF-kB signaling pathway.[11–13] Rhein protects IgAN nephropathy and 5/6 nephrectomized rats by inhibiting the TLR4 signaling pathway;[14,15] it can also alleviate renal interstitial fibrosis in rats by inhibiting the phosphorylation of STAT3 and thereby suppressing tubular cell apoptosis.[16] Formononetin protects rats from inflammation associated with cerebral ischemia-reperfusion injury by targeting the JAK2/STAT3 signaling pathway.[17] Furthermore, this study integrated network pharmacology with transcriptomics to accurately identify several key signaling pathways related to GQYS's therapeutic effects on IgAN, including the PI3K-AKT, AGE-RAGE, Toll-like receptor, TNF, NF-kB, cytokine-cytokine receptor interaction, and JAK-STAT signaling pathways. Based on the existing evidence for kaempferol, formononetin, and rhein, we further focused on and verified the TLR4/MyD88/NF-kB and IL-6/JAK2/STAT3 signaling pathways.

Toll-like receptors (TLRs) are identified to be potential mediators of innate immune response and inflammation.[18,19] TLRs, especially the TLR4 signaling pathway, have a critical role in mesangial cell injury and renal fibrosis by promoting the production of inflammatory markers in chronic kidney diseases, including IgAN.[20,21] Coppo et al reported elevated TLR4 expression in the peripheral blood mononuclear cells among individuals with IgAN.[22] He et al reported that TLR4 was markably upregulated in IgAN rats.[23] One of the canonical TLR4 signaling pathways is activating nuclear factor-kappa B (NF-kB) in a myeloid differentiation factor 88 (MyD88)-dependent manner, which subsequently stimulates the

https://doi.org/10.2147/DDDT.S526706

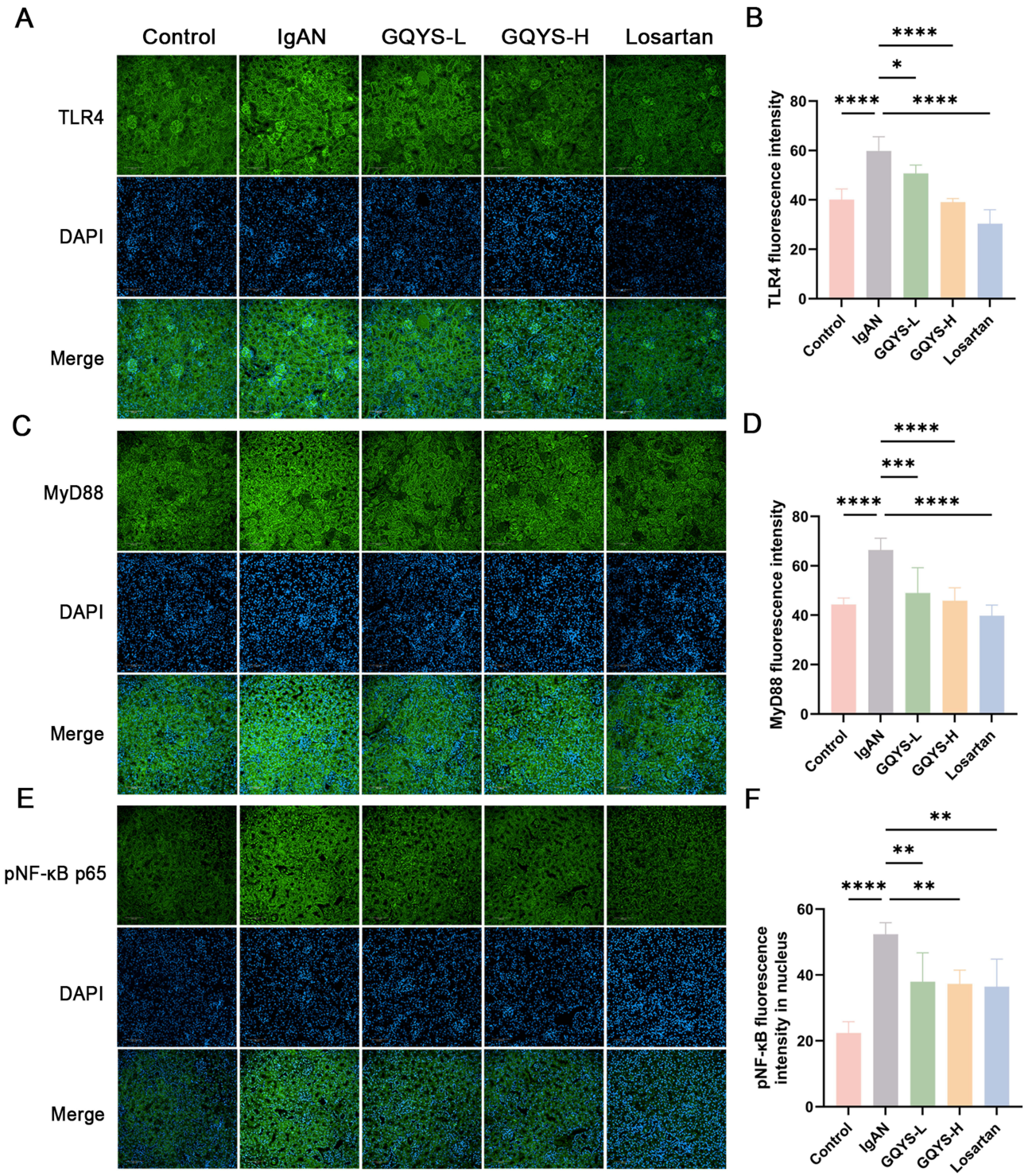

Figure 7 Detection of the TLR4/MyD88/NF-kB signaling pathway by immunostaining. Immunostaining of TLR4 (**A**), MyD88 (**C**), and pNF-kB (**E**) in each group, with nuclei stained by DAPI. Scale bars: 100 μm. The fluorescence intensity of TLR4 (**B**), MyD88 (**D**), and pNF-kB (**F**) were quantified using Image J (n=6). Data are presented as mean ± SD. The p-value indicates the statistical significance of each versus the IgAN group. *p < 0.05, **p < 0.01, ***p < 0.001, ****p < 0.0001.

expression of IL-6 and MCP-1. This indicates that the TLR4 signaling pathway may have a therapeutic effect for the alleviation of IgAN. In the Itgam-IRES-hCD89 mice, the TLR4/MyD88/NF-kB signaling pathway was upregulated significantly, and GQYS treatment decreased this occurrence, indicating that GQYS may alleviate IgAN through regulating TLR4/MyD88/NF-kB mediated inflammation.

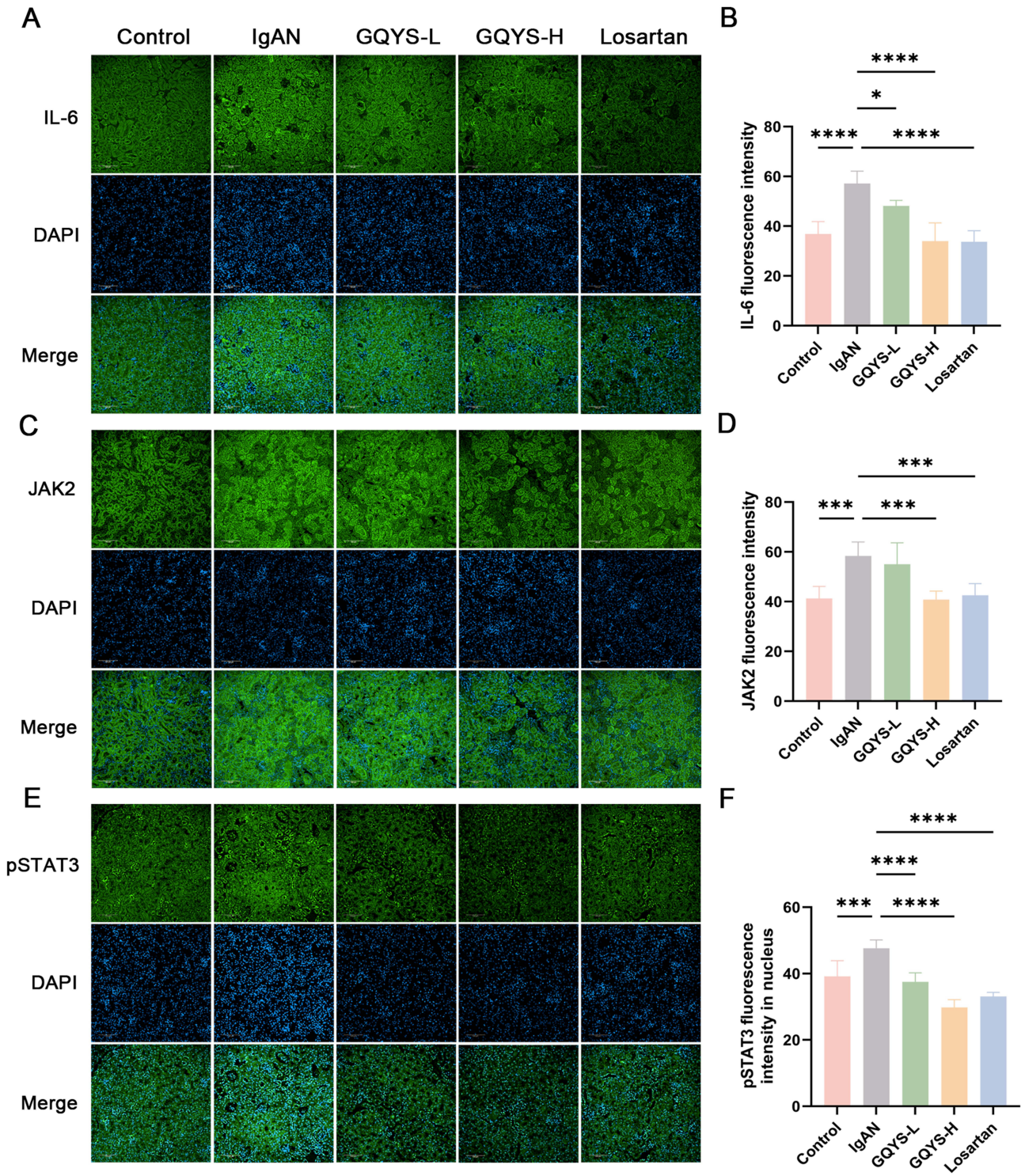

Figure 8 Detection of the IL-6/JAK2/STAT3 signaling pathway by immunostaining. Immunostaining of IL-6 (**A**), JAK2 (**C**), and pSTAT3 (**E**) in each group, with nuclei counterstained using DAPI. Scale bars: 100 μm. The fluorescence intensity of IL-6 (**B**), JAK2 (**D**), and pSTAT3 (**F**) were quantified using Image J (n=6). Data are presented as mean ± SD. The p-value indicates the statistical significance of each versus the IgAN group. *p < 0.05, ***p < 0.001, ****p < 0.0001.

Mounting evidence indicates that IL-6 is pivotal in IgAN pathogenesis.[24,25] Previous studies have indicated that IL-6 leads to elevated Gd-IgA1 synthesis in human cells that secrete IgA1, as well as in mouse IgAN models.[26–28] Highly-expressed renal IL-6 in IgAN is associated with the degree of IgA deposition and histologic damage.[29,30] Additionally, upregulated urinary IL-6 levels are closely associated with IgAN progression.[31,32] Among the downstream signaling pathways activated by IL-6, the JAK/STAT

https://doi.org/10.2147/DDDT.S526706

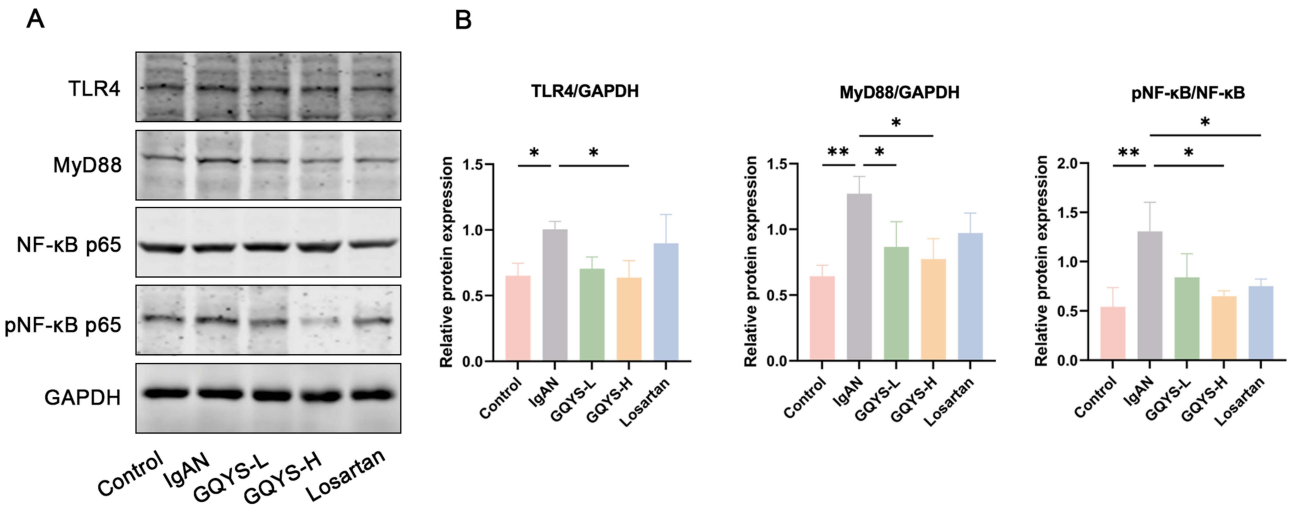

Figure 9 Detection of the TLR4/MyD88/NF-kB signal cascades by Western blotting. (**A**) The protein expression of TLR4, MyD88, and pNF-kB. (**B**) Relative protein level was calculated by grayscale analysis of target protein against GAPDH, respectively (n=6). Data are presented as mean ± SD. The p-value indicates the statistical significance of each versus the IgAN group. *p < 0.05, **p < 0.01.

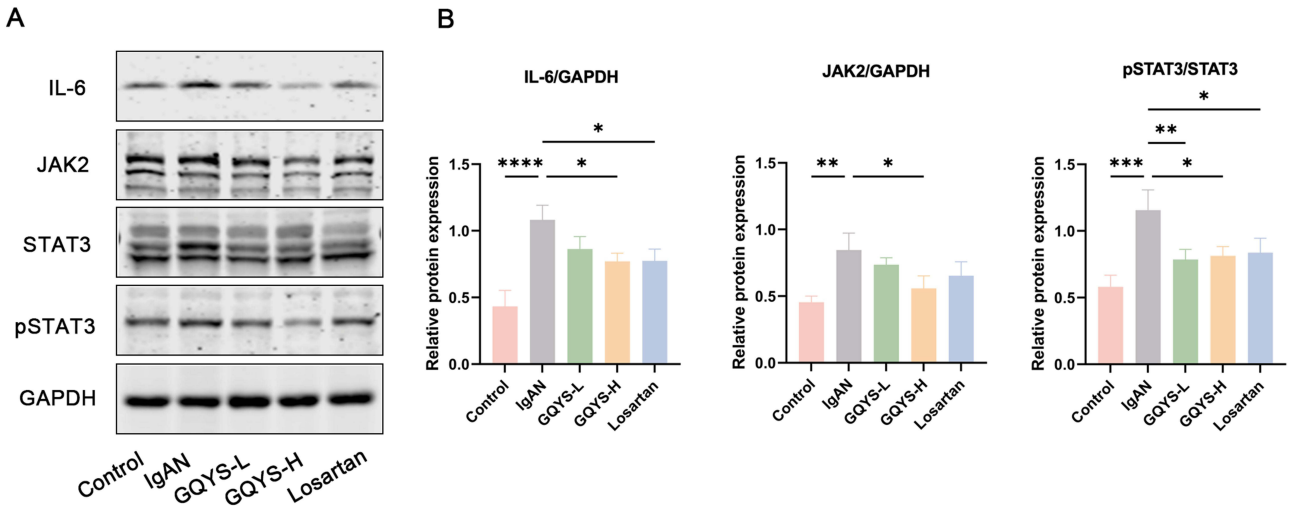

Figure 10 Detection of the IL-6/JAK2/STAT3 signal cascades by Western blotting. (**A**) The protein expression of IL-6, JAK2, and pSTAT3. (**B**) Relative protein level was calculated by grayscale analysis of target protein against GAPDH, respectively (n=6). Data are presented as mean ± SD. The p-value indicates the statistical significance of each versus the IgAN group. *p < 0.05, **p < 0.01, ***p < 0.001, ****p < 0.0001.

pathway is the most prominent. In our IgAN model, we observed a significant increase in the expression of proteins involved in the IL-6/JAK2/STAT3 signaling pathway, and treatment with GQYS decreased this occurrence. These results indicate that GQYS may reduce the inflammation and improve renal injury in IgAN mice by inhibiting the IL-6 signaling pathway.

There are some limitations in our study. First, inhibitors of related signaling pathways is lack for further verifying our findings. Second, no in vitro experiments with renal cells were performed in this study. Third, randomized clinical trial data on GQYS is currently unavailable, but our team is actively working on it. Notably, we have completed a retrospective study on 79 IgAN patients, showing that the GQYS significantly reduces serum creatinine and increases glomerular filtration rate (unpublished data). We hope to provide more data to support GQYS's clinical efficacy in the future.

Conclusion

The present study explores the therapeutic effect of GQYS on IgAN using a combination of network pharmacology and transcriptomics. Our results show GQYS may play a renoprotective role in IgAN through inhibiting TLR4/MyD88/NF-

kB and IL-6/JAK2/STAT3 signaling pathway. It is anticipated that this study may provide some theoretical basis for GQYS's development of new traditional Chinese medicine drugs and suggest promising translational prospects for treating IgAN patients.

Abbreviations

GQYS, Gui-qi-yi-shen; IgAN, IgA nephropathy; PAS, Periodic Acid-Schiff; ESRD, end-stage kidney disease; TCMSP, Traditional Chinese Medicine systems pharmacology database and analysis platform; TLRs, toll-like receptors; MyD88, myeloid differentiation factor 88; UPLC-Q-TOF-MS/MS, ultra-high-performance liquid chromatography with quadrupole time-of-flight mass spectrometry; ESI, electrospray ionization; PPI, protein-protein interaction; ALT, alanine aminotransferase; AST, aspartate aminotransferase; IF, immunofluorescence; GQYS-L, low-dose GQYS; GQYS-H, high-dose GQYS; TLR, Toll-like receptor signaling; TNF, Tumor necrosis factor; NF-kB, nuclear factor-kappa B; DEGs, differentially expressed genes; SD, standard deviation.

Data Sharing Statement

Data will be made available on request.

Author Contributions

All authors made a significant contribution to the work reported, whether that is in the conception, study design, execution, acquisition of data, analysis and interpretation, or in all these areas; took part in drafting, revising or critically reviewing the article; gave final approval of the version to be published; have agreed on the journal to which the article has been submitted; and agree to be accountable for all aspects of the work.

Funding

This work was supported by the Hangzhou Municipal Health Commission Project (A20231285), the financial Support for Top notch Medical and Health Youth Talents in Hangzhou City (Feng Wan), Key Laboratory of Precise Prevention, Treatment of Rheumatism Syndrome of renal Wind Disease (GZY-ZJ-SY-2305), and Peak Discipline Nephrology of Hangzhou (Integrated Traditional and Western Medicine, 2025HZGF12).

Disclosure

The authors declare that there is no competing interest regarding the publication of this paper.

References

1. Selvaskandan H, Barratt J, Cheung CK. Novel treatment paradigms: primary IgA nephropathy. *Kidney Int Rep*. 2024;9(2):203–213. doi:10.1016/j.ekir.2023.11.026
2. Floege J, Bernier-Jean A, Barratt J, Rovin B. Treatment of patients with IgA nephropathy: a call for a new paradigm. *Kidney Int*. 2025;107(4):640–651. doi:10.1016/j.kint.2025.01.014
3. Cheung CK, Alexander S, Reich HN, Selvaskandan H, Zhang H, Barratt J. The pathogenesis of IgA nephropathy and implications for treatment. *Nat Rev Nephrol*. 2025;21(1):9–23. doi:10.1038/s41581-024-00885-3
4. Ma S, Zhao M, Chang M, Shi X, Zhang Y, Shi Y. Effects and mechanisms of Chinese herbal medicine on IgA nephropathy. *Phytomedicine*. 2023;117:154913. doi:10.1016/j.phymed.2023.154913
5. Wang XH, Lang R, Liang Y, Zeng Q, Chen N, Yu RH. Traditional Chinese Medicine in treating IgA nephropathy: from basic science to clinical research. *J Transl Int Med*. 2021;9(3):161–167. doi:10.2478/jtim-2021-0021
6. Bao Z, Zhu C, Sun Y, Liao J, Chen H. Effects of Centella Asiatica Compound on renal expression of TNF-α and MIF in rats with IgA nephropathy. *China J Tradition Chinese Med Pharm*. 2019;34(08):3731–3735.
7. Chen Y, Min J, Wu M, Yang R, Yu D. Therapeutic effect of the compound centella asiatica in patients with stages 4-5 CKD and its influence on serum α-Klotho and FGF23 levels. *Clin Trad Med Pharmacol*. 2025;6(1):200202. doi:10.1016/j.ctmp.2025.200202
8. Launay P, Grossetete B, Arcos-Fajardo M, et al. Fcalpha receptor (CD89) mediates the development of immunoglobulin A (IgA) nephropathy (Berger's disease). Evidence for pathogenic soluble receptor-Iga complexes in patients and CD89 transgenic mice. *J Exp Med*. 2000;191(11):1999–2009. doi:10.1084/jem.191.11.1999
9. Wehbi B, Pascal V, Zawil L, Cogne M, Aldigier JC. History of IgA nephropathy mouse models. *J Clin Med*. 2021;10(14). doi:10.3390/jcm10143142
10. Nair AB, Jacob S. A simple practice guide for dose conversion between animals and human. *J Basic Clin Pharm*. 2016;7(2):27–31. doi:10.4103/0976-0105.177703

11. Kadioglu O, Nass J, Saeed ME, Schuler B, Efferth T. Kaempferol is an anti-inflammatory compound with activity towards NF-kappaB pathway proteins. *Anticancer Res*. 2015;35(5):2645–2650.
12. Hosseini A, Alipour A, Baradaran Rahimi V, Askari VR. A comprehensive and mechanistic review on protective effects of kaempferol against natural and chemical toxins: role of NF-kappaB inhibition and Nrf2 activation. *Biofactors*. 2023;49(2):322–350. doi:10.1002/biof.1923
13. Park MJ, Lee EK, Heo HS, et al. The anti-inflammatory effect of kaempferol in aged kidney tissues: the involvement of nuclear factor-kappaB via nuclear factor-inducing kinase/IkappaB kinase and mitogen-activated protein kinase pathways. *J Med Food*. 2009;12(2):351–358. doi:10.1089/jmf.2008.0006
14. Liu M, Wang L, Wu X, et al. Rhein protects 5/6 nephrectomized rat against renal injury by reducing inflammation via NF-kappaB signaling. *Int Urol Nephrol*. 2021;53(7):1473–1482. doi:10.1007/s11255-020-02739-w
15. Chen X, Peng S, Zeng H, Fu A, Zhu Q. Toll-like receptor 4 is involved in a protective effect of rhein on immunoglobulin A nephropathy. *Indian J Pharmacol*. 2015;47(1):27–33. doi:10.4103/0253-7613.150319
16. Chen Y, Mu L, Xing L, Li S, Fu S. Rhein alleviates renal interstitial fibrosis by inhibiting tubular cell apoptosis in rats. *Biol Res*. 2019;52(1):50. doi:10.1186/s40659-019-0257-0
17. Yu L, Zhang Y, Chen Q, et al. Formononetin protects against inflammation associated with cerebral ischemia-reperfusion injury in rats by targeting the JAK2/STAT3 signaling pathway. *Biomed Pharmacother*. 2022;149:112836. doi:10.1016/j.biopha.2022.112836
18. Coppo R, Amore A, Peruzzi L, Vergano L, Camilla R. Innate immunity and IgA nephropathy. *J Nephrol*. 2010;23(6):626–632.
19. Lee M, Suzuki H, Ogiwara K, et al. The nucleotide-sensing toll-like receptor 9/toll-like receptor 7 system is a potential therapeutic target for IgA nephropathy. *Kidney Int*. 2023;104(5):943–955. doi:10.1016/j.kint.2023.08.013
20. Zou JN, Xiao J, Hu SS, et al. Toll-like receptor 4 signaling pathway in the protective effect of pioglitazone on experimental immunoglobulin A nephropathy. *Chin Med J*. 2017;130(8):906–913. doi:10.4103/0366-6999.204101
21. Liusheng LI, Mingming Z, Meiying C, et al. Protective effect of modified Huangqi Chifeng decoction on immunoglobulin A nephropathy through toll-like receptor 4/myeloid differentiation factor 88/nuclear factor-kappa B signaling pathway. *J Tradit Chin Med*. 2024;44(2):324–333. doi:10.19852/j.cnki.jtcm.20240203.001
22. Coppo R, Camilla R, Amore A, et al. Toll-like receptor 4 expression is increased in circulating mononuclear cells of patients with immunoglobulin A nephropathy. *Clin Exp Immunol*. 2010;159(1):73–81. doi:10.1111/j.1365-2249.2009.04045.x
23. He L, Peng X, Liu G, et al. Anti-inflammatory effects of triptolide on IgA nephropathy in rats. *Immunopharmacol Immunotoxicol*. 2015;37(5):421–427. doi:10.3109/08923973.2015.1080265
24. Groza Y, Jemelkova J, Kafkova LR, Maly P, Raska M. IL-6 and its role in IgA nephropathy development. *Cytokine Growth Factor Rev*. 2022;66:1–14. doi:10.1016/j.cytogfr.2022.04.001
25. Taniguchi Y, Yorioka N, Kumagai J, et al. Interleukin-6 localization and the prognosis of IgA nephropathy. *Nephron*. 1999;81(1):94–98. doi:10.1159/000045254
26. Suzuki H, Raska M, Yamada K, et al. Cytokines alter IgA1 O-glycosylation by dysregulating C1GalT1 and ST6GalNAc-II enzymes. *J Biol Chem*. 2014;289(8):5330–5339. doi:10.1074/jbc.M113.512277
27. Yamada K, Huang ZQ, Raska M, et al. Inhibition of STAT3 signaling reduces IgA1 autoantigen production in IgA nephropathy. *Kidney Int Rep*. 2017;2(6):1194–1207. doi:10.1016/j.ekir.2017.07.002
28. Makita Y, Suzuki H, Kano T, et al. TLR9 activation induces aberrant IgA glycosylation via April- and IL-6-mediated pathways in IgA nephropathy. *Kidney Int*. 2020;97(2):340–349. doi:10.1016/j.kint.2019.08.022
29. Rops A, Jansen E, van der Schaaf A, et al. Interleukin-6 is essential for glomerular immunoglobulin A deposition and the development of renal pathology in Cd37-deficient mice. *Kidney Int*. 2018;93(6):1356–1366. doi:10.1016/j.kint.2018.01.005
30. Lim CS, Yoon HJ, Kim YS, et al. Clinicopathological correlation of intrarenal cytokines and chemokines in IgA nephropathy. *Nephrology*. 2003;8(1):21–27. doi:10.1046/j.1440-1797.2003.00128.x
31. Zhao W, Feng S, Wang Y, et al. Elevated urinary IL-6 predicts the progression of IgA nephropathy. *Kidney Int Rep*. 2023;8(3):519–530. doi:10.1016/j.ekir.2022.12.023
32. Harada K, Akai Y, Kurumatani N, Iwano M, Saito Y. Prognostic value of urinary interleukin 6 in patients with IgA nephropathy: an 8-year follow-up study. *Nephron*. 2002;92(4):824–826. doi:10.1159/000065465